Simulating Impedance Spectra from a Mechanistic Point of View: Application to Zinc Dissolution

Elisabet Ahlberg* and Helge Anderson

Department of Inorganic Chemistry, Chalmers University of Technology and University of Göteborg, S-412 96 Göteborg, Sweden

Ahlberg, E. and Anderson, H., 1992. Simulating Impedance Spectra from a Mechanistic Point of View: Application to Zinc Dissolution. – Acta Chem. Scand. 46: 15–24.

The dissolution of zinc in slightly acidic perchlorate and chloride solutions has been studied using potentiodynamic sweeps and impedance spectroscopy. The experimental data are compared with simulated data derived from the suggested mechanism. The Tafel slope of the potentiodynamic sweeps changes from ca. 60 to 30 mV upon addition of hydroxide or chloride ions. The impedance spectra show three relaxations interpreted as charge transfer at high frequencies and relaxation of two adsorbed intermediates at low frequencies. Based on these experimental results a model for the zinc dissolution is presented. The main dissolution path is autocatalytic with one adsorbed intermediate. There is a parallel path of less importance which includes one additional adsorbed intermediate. The effect of hydroxide and chloride ions is explained by a destabilization of the adsorbed intermediate occuring in the autocatalytic path.

One of the most important applications of zinc is its use as a protective coating against corrosion on steel for outdoor use.[1] There are two main reasons why zinc coatings are especially good to protect steel agains corrosion. (1) Zinc itself is resistant to attack in a normal atmosphere through the formation of insoluble zinc carbonates. (2) Zinc is considerably more electronegative than iron, and thus the cathodic protection of steel will result.

In recent years the use of galvanized steel in the automotive industry has stimulated research into the underfilm corrosion of painted steel. The mechanism of propagation was suggested to be anodic initially for all types of systems. In the propagation area zinc is thus dissolved into the electrolyte, causing the pH to drop to slightly acidic values. The effects of variables such as the type of coating (zinc or zinc alloys), the metal coating thickness, the test conditions and the phosphating system have been studied.[2,3]

The corrosion of zinc has been the subject of numerous publications, but the detailed mechanism of the dissolution of polycrystalline zinc is still not fully understood.[4-16] The hypothesis of a monovalent zinc ion existing as an adsorbed intermediate on the electrode surface seems to be well established today.[8-16] The most simple mechanism involving one adsorbed intermediate can be written as steps (1) and (2). The reaction proceeds via two consecutive

$$\text{Zn} \underset{k_{-1}}{\overset{k_1}{\rightleftharpoons}} \text{Zn}^+{}_{ad} + e^- \tag{1}$$

$$\text{Zn}^+{}_{ad} \overset{k_2}{\longrightarrow} \text{Zn}^{2+}{}_{aq} + e^- \tag{2}$$
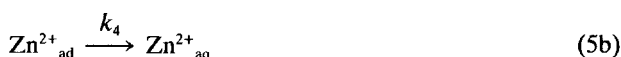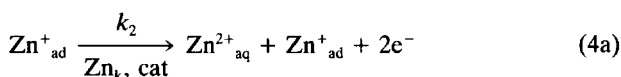
---

* To whom correspondence should be addressed.

electron-transfer steps, of which the first is assumed to be in equilibrium. The most common evidence for this mechanism is steady-state polarization curves, which show a Tafel slope of 40 mV ($\alpha = 1/2$). This was found experimentally by, for example, Hurlen[9] and Heusler.[11]

It is well known that anions such as the halogens increase the dissolution rate of zinc.[4,5,11] However, there seems to be some uncertainty whether this effect is caused by a change in the double-layer structure (specific adsorption) or if the anions undergo complex formation with Zn^{2+}. In an early paper[5] Hurlen suggested that the chloride ions do not directly participate in the dissolution reaction. However, in a later paper[9] he concluded that, at high chloride concentrations ($[\text{Cl}^-] > 1$ M), the dichloro-complex $\text{ZnCl}_2{}^-/\text{ZnCl}_2$ couple are the electroactive species, whereas at low chloride concentrations a species with one or no chloride ligand is electroactive. Similar results were obtained by Blackledge and Hush,[4] who studied the effect of Cl^-, Br^-, I^- and SCN^- on the $\text{Zn(Hg)}/\text{Zn}^{2+}$ electrode. The reaction order with respect to these anions was found to be close to one except for I^- at high concentrations, where the reaction order was two. However, these authors did not exclude the possibility of specific adsorption of these ions, which may have altered the double-layer structure and thereby increased the reaction rate.

Impedance spectroscopy (IS) is now a common and useful technique for studying metal dissolution reactions. One of its advantages is the possibility of studying the relaxation of adsorbed intermediates. Results obtained from IS measurements by Cachet and Wiart in chloride solution[14,15] and by Deslouis in sulfate solution[16] indicate that several adsorbed intermediates may participate in the dissolution reaction of zinc. These studies have led to an alternative

formulation of the dissolution mechanism. It includes an autocatalytic step, (4a) in the reaction scheme below, similar to that proposed by Heusler for the dissolution of iron.[12]

$$Zn \underset{k_{-1}}{\overset{k_1}{\rightleftharpoons}} Zn^+_{ad} + e^- \quad (3)$$

$$Zn^+_{ad} \xrightarrow[Zn_k, \text{ cat}]{k_2} Zn^{2+}_{aq} + Zn^+_{ad} + 2e^- \quad (4a)$$

$$Zn^+_{ad} \xrightarrow{k_3} Zn^{2+}_{ad} + e^- \quad (4b)$$

$$Zn^{2+}_{ad} \xrightarrow{k_4} Zn^{2+}_{aq} \quad (5b)$$

The monovalent zinc species produced in the first step is further oxidized either through the autocatalytic path (a) or the noncatalytic path (b). The autocatalytic path requires the presence of a kink step and does not consume any Zn^+_{ad} species. It is supposed to be a simultaneous two-electron transfer. The other path, which was found to be of minor importance in these studies,[14-16] includes a second adsorbed species Zn^{2+}_{ad} which is chemically dissolved into the solution.

In a recent paper[17] we presented a theoretical study of the impedance and polarization behaviour of some typical dissolution mechanisms of metals. The effect of chemical and catalytic steps on the impedance was investigated. It was shown that for mechanisms with two or more adsorbed intermediates there is no unambiguous relationship between the experimental time constants, obtained from the spectrum, and the time constants found from the mechanistic model. It was also shown that for mechanisms involving pure chemical steps the ln $(10)R_pI_{ss}$ product cannot always be used as a Tafel value.

In the present paper the mechanism of zinc dissolution in slightly acidic electrolytes has been studied. Also, the effect of anions normally detected in corrosion products of specimens tested outdoors, such as chloride and hydroxide, has been studied. Electrochemical techniques such as potentiodynamic sweeps and impedance spectroscopy have been used to elucidate the detailed mechanism of zinc dissolution. The experimental data are compared to simulated data based on the proposed mechanism. The main dissolution route is autocatalytic, regardless of the electrolyte composition. The effect of anions is explained by a destabilization of Zn^+_{ad}.

Experimental

Instrumentation, cells and electrodes. A PAR (Princeton Applied Research) 173 potentiostat with a model 276 interface and a HP 85B computer, printer and plotter were used for generation and recording of polarization curves. A Solartron 1174 frequency response analyser coupled to the PAR potentiostat was used for impedance measurements.

Serious phase shifts in the high-frequency region could be avoided by applying the procedure proposed by Kendig et al.[18] Programs for measuring the impedance were developed.[19] Ohmic compensation was achieved by measuring the ohmic resistance between the working electrode and the reference electrode by impedance measurements. Data were mathematically compensated for iR drop on plotting.

The cell was a Metrohm titration vessel with a specially designed lid. A calomel reference electrode with saturated NaCl solution, $E = 0.236$ V vs. NHE, and a platinum counter-electrode were used throughout the work. The electrolyte solution was bubbled with purified nitrogen for at least 40 min before the experiment, and a nitrogen atmosphere was maintained in the cell during the experiments.

Rotating disc electrodes with a surface of 0.2 or 0.03 cm² were prepared from 99.99 % pure zinc rods (Johnson Matthey). The electrodes were moulded in epoxy, exposing only the circular disc surface.

Chemicals. 1 M sodium perchlorate was prepared from p.a. NaClO₄ (Merck) and doubly distilled water. The pH of the solution was adjusted by addition of perchloric acid or sodium hydroxide of the same ionic strength as the electrolyte. The pH was controlled by a Radiometer pH-stat system (pH-meter 84, titrator TTT 80 and autoburette ABU 80) together with a combined glass electrode (GK 2401c).

Pre-treatment. Before each experiment the electrode was wet-ground on silicon carbide paper (1000 and 4000 mesh), rinsed with doubly distilled water and immediately placed in the deoxygenated solution. The electrode was pre-activated before each series of measurements by three polarization sweeps, in which each sweep consisted of the following voltage ramps: ramp 1: rest potential to −800 mV (positive direction); ramp 2: −800 to −1200 mV; ramp 3: −1200 to −800 mV. All potentials are given with respect to the saturated sodium calomel electrode, SSCE.

Polarization measurements. Each experiment was carried out in a series of polarization sweeps in which each sweep was followed by a change in one of the experimental parameters (i.e. the electrolyte composition or the rotation speed of the electrode). After each change the system was allowed to reach a stable rest potential before the next sweep was carried out. The sweep rate was always 2 mV s⁻¹. This rate was shown, by studies at different sweep rates, to be slow enough to maintain steady-state conditions at the electrode surface. The sweeps consisted of the same voltage ramps as in the preactivation routine. The rotation speed of the electrode was 30 rev. s⁻¹, except in the experiments where the influence of this parameter was studied.

Impedance measurements. Before each series of impedance measurements, the electrode was preactivated with polarization sweeps as described earlier. The system was then

allowed to reach steady state for at least 3 min at the measuring potential before the impedance was recorded. Data were collected from 50 kHz down to 10 mHz with 10 points per decade of frequency. For each solution the experiments were performed sequentially at different potentials, stepwise. The preactivation routine was not performed between these measurements. The rotation speed of the electrode was the same as in the polarization measurements, 30 rev. s^{-1}.

Results

Tafel plots of the polarization curves, which show good linearity in a current range of at least two decades in the anodic region, have been used in the analysis of the data. Since the current in the Tafel region was shown to be independent of the rotation speed of the electrode, we assume that the reactions are kinetically controlled and that they exhibit Tafel behaviour.

Polarization measurements. Fig. 1(a) shows typical polarization curves of zinc in perchlorate solutions of dif-
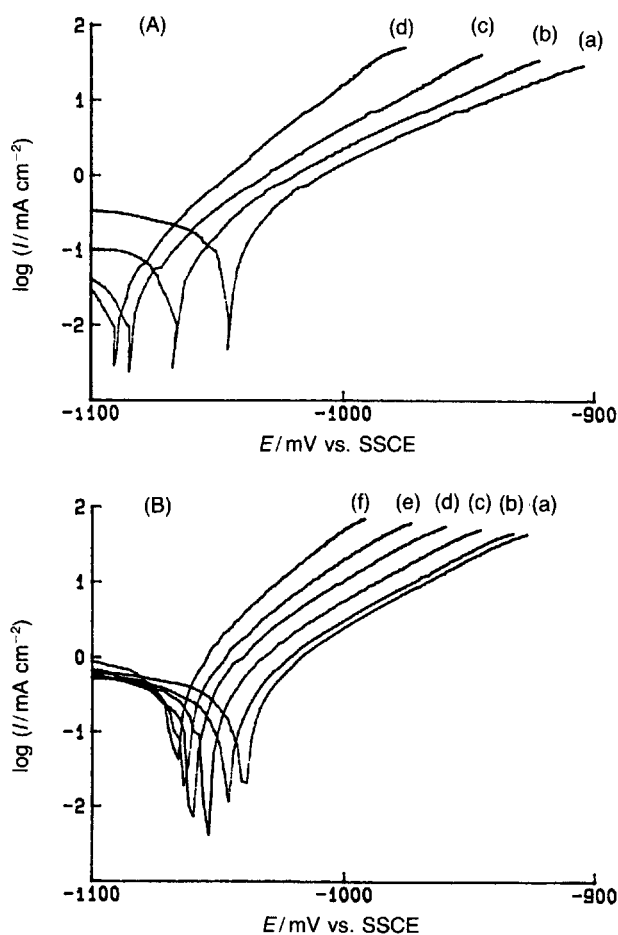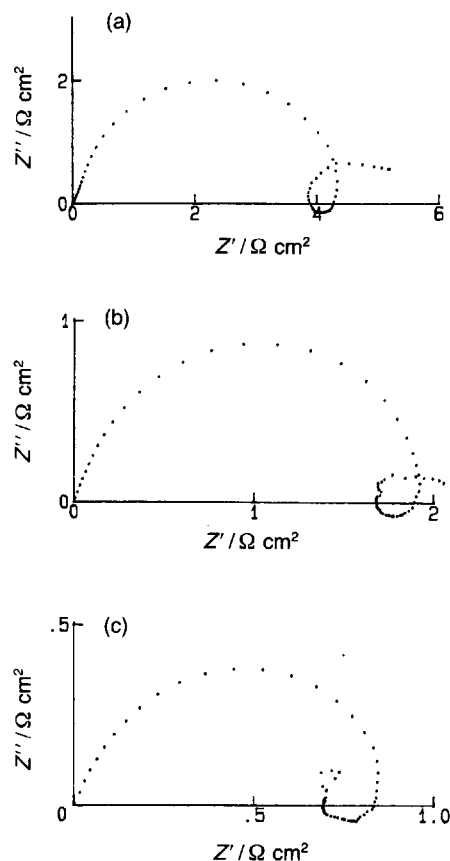

Fig. 2. Experimental impedance spectra of zinc in 1 M $NaClO_4$ at pH 3 at three anodic potentials: (a) 45, (b) 65 and (c) 95 mV from the rest potential.

Fig. 1. Experimental polarization curves of zinc. (A) 1 M $NaClO_4$: (a) pH 3.0, (b) 3.5, (c) 4.0 and (d) 4.5. (B) x M NaCl in $(1 - x)$ M $NaClO_4$ at pH 3: (a) $x = 0$, (b) 0.01, (c) 0.03, (d) 0.1, (e) 0.3 and (f) 1.0 mol dm^{-3}.

ferent pH values, ranging from 3.0 to 4.5. At pH 3 the anodic Tafel slope of the polarization curve lies in the range 60 ± 4 mV. As the pH of the electrolyte is increased, the Tafel slope gradually decreases towards 30 mV at pH 4.5. These experiments showed good reproducibility and were independent of the direction of the pH change in the series of experiments.

In Fig. 1(b) the effect of chloride ions on the zinc dissolution is shown. The polarization curves were obtained at pH 3. At low concentrations (<0.01 M) there are no or very small changes in the polarization curve. At higher chloride concentrations there is a shift of the Tafel slope from the initial value down to approximately 30–35 mV.

Impedance measurements. Figs. 2–4 show the impedance plots of measurements performed in 1 M $NaClO_4$ at pH 3.0 [Figs. 2(a)–(c)], at pH 5.0 [Figs. 3(a)–(c)] and in 1 M NaCl at pH 3.0 [Figs. 4(a)–(c)]. Three relaxations are observed in all spectra except the one obtained at high overpotentials in $NaClO_4$ at pH 3.0, where only two relaxations are observed [Fig. 2(c)]. The capacitive loop in the high-frequency region of the spectra is associated with the charge-transfer process, and the other two, one inductive and one capacitive, are interpreted as relaxations of intermediates
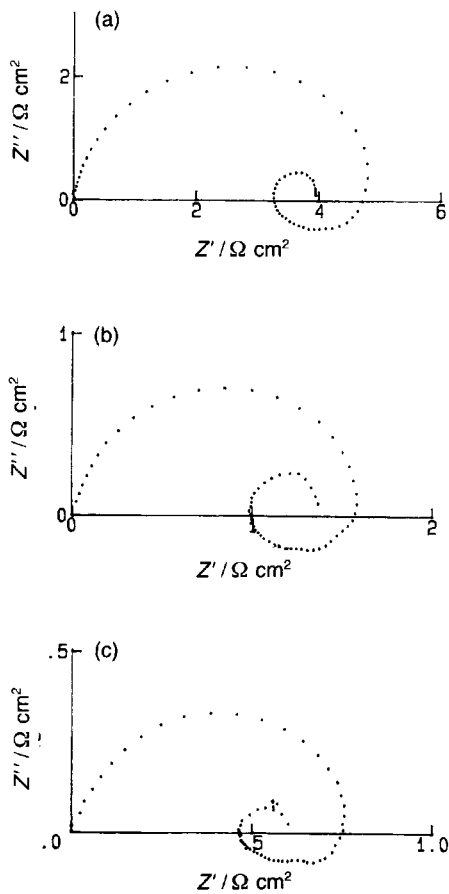
Fig. 3. Experimental impedance spectra of zinc in 1 M NaClO$_4$ at pH 5 at three anodic potentials: (a) 45, (b) 65 and (c) 95 mV from the rest potential.
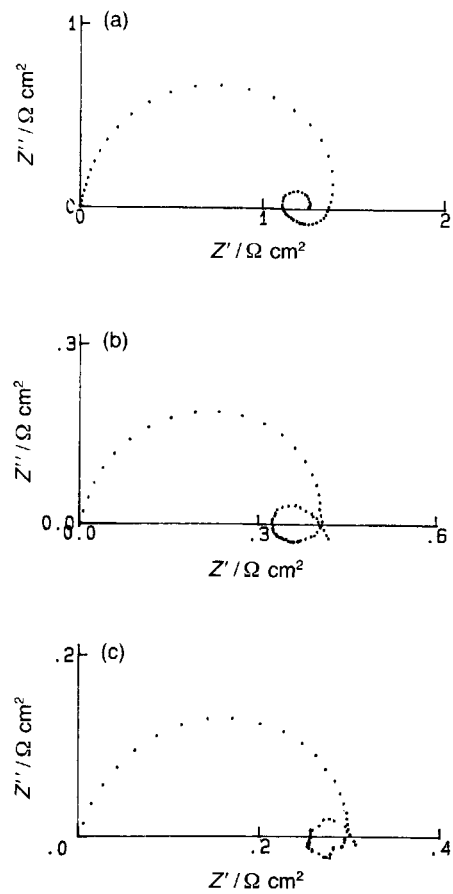

Fig. 4. Experimental impedance spectra of zinc in 1 M NaCl at pH 3 at three anodic potentials: (a) 40, (b) 60 and (c) 75 mV from the rest potential.

adsorbed on the electrode surface. Parameters evaluated from these spectra are listed in Table 1.

The charge-transfer resistance is obtained from the diameter of the charge-transfer loop, and the potential dependence of the time constants has been estimated through the maxima or minima of the imaginary part of the impedance. This may cause some errors if the time con-

stants are not well separated.[17] However, by applying the same procedure on the simulated spectra the quantities evaluated are comparable to each other.

Figs. 2(a)–(c) show the impedance behaviour of zinc in 1 M NaClO$_4$ at pH 3.0 at three overpotentials (45, 65 and 90 mV) versus the rest potential in the solution. The steady-state current obtained from the impedance meas-

Table 1. Parameters evaluated from the experimental impedance spectra at various anodic potentials.

$E - E_{rest}$/mV	I_{ss}/mA cm^{-2}	R_{ct}/Ω cm^2	R_p/Ω cm^2	τ_1/10^{-2} s	τ_2/s
45[a]	4.4	4.3	5.2	8.4	3.2
65[a]	15	1.9	2.1	2.5	3.2
95[a]	38	0.85		1.8	
45[b]	4.6	4.9	3.9	1.5	2.0
65[b]	16	1.6	1.4	1.5	4.0
95[b]	41	0.77	0.60	1.0	2.5
40[c]	11	1.4	1.3	2.1	2.0
60[c]	33	0.42	0.41	2.0	1.0
75[c]	64	0.30	0.31	1.3	1.0

[a][ClO$_4^-$] = 1 mol dm^{-3}, [Cl$^-$] = 0 mol dm^{-3}, pH 3.0. [b][ClO$_4^-$] = 1 mol dm^{-3}, [Cl$^-$] = 0 mol dm^{-3}, pH 5.0. [c][ClO$_4^-$] = 0 mol dm^{-3}, [Cl$^-$] = 1 mol dm^{-3}, pH 3.0.

urement is slightly higher than that from the polarization sweep measurement. The potential dependence of the time constant of the inductive loop, τ_1, is rather strong, 50 mV per decade. The other time constant, τ_2, associated with the capacitive loop in the low-frequency part of the spectra obtained at 45 and 65 mV, is approximately 3 s.

Figs. 3(a)–(c) show the impedance spectra obtained in 1 M $NaClO_4$ at pH 5. The lower Tafel slope obtained in the polarization measurement in this solution is reflected in a slightly stronger potential dependence of the charge-transfer resistance. It may be noted that the potential dependence of τ_1 is considerably weaker compared to the measurement at pH 3. Even if the uncertainty in the estimations of these time constants is taken into account, there is a clear tendency towards a less potential dependence of τ_1 at pH 5. The diameter of the capacitive loop in the low-frequency region was found to be smaller and does not intersect the charge-transfer loop as it does at pH 3. The time constant, τ_2, is of the same order as in the pH 3 solution and does not show any regular variation with the potential. At larger overpotentials [Figs. 3(b) and (c)] there is a weak indication of an additional inductive relaxation. This might be due to the formation of insoluble zinc hydroxide species, which can be formed at this pH.

The results from the impedance measurements in 1 M NaCl solution at pH 3.0 are shown in Figs. 4(a)–(c). As expected, the charge-transfer resistance obtained in this solution is smaller than in perchlorate solution. The potential dependence of τ_1 is lower than in the perchlorate solution at the same pH. The time constant for the capacitive loop, τ_2, did not show any significant variation with the potential.
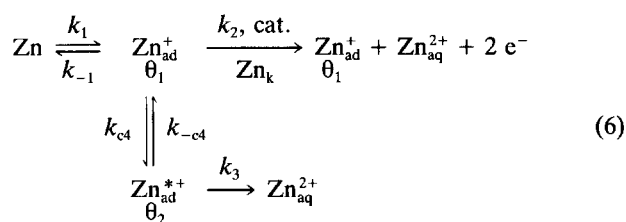
It is worth noting the similarities between the results obtained in the chloride solution and the perchlorate solution at pH 5. In both these solutions the same type of Tafel behaviour of the polarization curve was observed ($b_a = 30$–35 mV), which differed markedly from the results obtained in perchlorate solution at pH 3 ($b_a = 60 \pm 4$ mV). The potential dependence of τ_1 was found to be the same as in perchlorate solution at pH 5. From these experimental results we conclude that the hydroxide and chloride ions have similar effects on the dissolution reaction of zinc. These findings will be utilized in the discussion section.

Simulation of the results. A computer program was developed in order to simulate our experimental polarization curves and impedance spectra. The derivation of the impedance has been described in more detail elsewhere.[17] At least 20 different dissolution routes were formulated and tested with different sets of rate constants. No concern was taken of the cathodic reactions, since all the experiments were carried out in the anodic region sufficiently far from the rest potential. The criteria we stated for a mechanism to be regarded as possible were as follows: (1) The shape and the characteristics of the simulated spectra should agree with the experimental ones over an acceptably wide range of potentials. (2) The mechanism should explain the change

of the Tafel slope obtained when the concentration of chloride or hydroxide ions was increased. (3) The mechanism should explain the experimental potential dependences of the time constants.

Some of the mechanisms could be excluded more or less from their steady-state characteristics. The rest were extensively examined in the simulation program. The rate constants used are the normalized rate constants, which are the product of the heterogeneous rate constant, k_n^o, in cm s^{-1} and the concentration of the reacting species in mol cm^{-3}. The normalized rate constants, in which the concentrations of chloride ions and hydroxide ions are taken into account (k_1^o, k_{-1}^o and k_2^o), are divided into two parts. The first part corresponds to zero concentration of the anions. The second part contains the contribution from anions and is written as the activity of the species in the solution multiplied by a scaling factor, $f_{n,x}$, in cm^3 mol^{-1}. The scaling factor was adjusted so that the effects of the anions in the simulated data took place in the same concentration range as in the experimental observations. In order to make the experimental and simulated results comparable, the evaluation of the time constants in the simulated spectra was performed in the same way as in the experimental spectra described earlier.

The mechanism that showed the best agreement with experimental data was Scheme (6), where the potential-

$$\text{Zn} \underset{k_{-1}}{\overset{k_1}{\rightleftharpoons}} \underset{\theta_1}{\text{Zn}_{ad}^+} \xrightarrow[\text{Zn}_k]{k_2, \text{ cat.}} \underset{\theta_1}{\text{Zn}_{ad}^+} + \text{Zn}_{aq}^{2+} + 2\ e^-$$

$$k_{c4} \Big\Vert k_{-c4} \tag{6}$$

$$\underset{\theta_2}{\text{Zn}_{ad}^{*+}} \xrightarrow{k_3} \text{Zn}_{aq}^{2+}$$

independent steps are indicated by 'c' in the rate constant. The parameters obtained from the simulation of this mechanism are listed in Table 2. The main dissolution path depends on both the potential and the concentration of anions. The anodic polarization and the presence of anions both favoured the catalytic path, denoted 'cat' in the scheme. The parallel path includes one additional adsorbed intermediate, Zn_{ad}^{+*}. The relaxation of the adsorbed Zn_{ad}^+ species is associated with the inductive loop in the experimental spectra and the Zn_{ad}^{+*} species with the capacitive loop. The catalytic path of this mechanism has already been suggested as a route for zinc dissolution by Cachet and Wiart[15] and later by Deslouis et al.[16] The reaction of the adsorbed Zn_{ad}^+ intermediate formed in the first step is catalysed by the presence of kink sites in the zinc lattice. The Zn atom in this kink site, Zn_k, is simultaneously oxidised to Zn_{ad}^+. Thus, the number of electrons transferred in the autocatalytic step is two. The presence of this catalytic step influences both the steady-state polarization curve and the impedance spectrum compared with the simple non-catalytic mechanism mentioned in the introduction. The Tafel slope is changed from 40 or 120 mV to 30 or 60 mV,

Table 2. Parameters evaluated from the simulated impedance spectra at different anodic potentials.

$E - E_{rest}$/mV	I_{ss}/mA cm^{-2}	R_{ct}/Ω cm^2	R_p/Ω cm^2	τ_1/10^{-2} s	τ_2/s
45[a]	6.3	4.1	4.4	13	2.2
65[a]	16	1.7	1.9	9.0	1.9
90[a]	50	0.52	0.62	5.6	1.6
45[b]	3.9	5.5	3.9	3.5	5.8
65[b]	13	1.9	1.5	3.8	4.6
90[b]	50	0.52	0.46	4.3	3.4
40[c]	11	2.1	1.6	3.4	4.3
60[c]	33	0.77	0.69	3.7	3.3
75[c]	70	0.37	0.36	3.9	2.7

[a][ClO$_4^-$] = 1 mol dm^{-3}, [Cl$^-$] = 0 mol dm^{-3}, pH 3.0. [b][ClO$_4^-$] = 1 mol dm^{-3}, [Cl$^-$] = 0 mol dm^{-3}, pH 5.0. [c][ClO$_4^-$] = 0 mol dm^{-3}, [Cl$^-$] = 1 mol dm^{-3}, pH 3.0.

depending on the rate-determining step and the degree of coverage of the intermediate. As a result, the potential dependence of the charge-transfer resistance becomes stronger. Thus, the steady-state behaviour observed in the experiments strongly suggests a catalytic dissolution route where a Tafel slope of 30 or 60 mV in the limiting potential regions is predicted. The parallel and non-catalytic path proceeds, in contrast to the model of Cachet and Wiart, via a Zn_{ad}^{+*} species formed chemically from Zn_{ad}^+. The Zn_{ad}^{+*} species is then further oxidised to Zn_{aq}^{2+}. The existence of the Zn_{ad}^{+*} species is hypothetical. It is introduced in order to explain the potential-independent capacitive loop in the low-frequency part of the spectra. The relevance of such a species will be discussed.

Fig. 5(a) shows the simulated polarization curve which corresponds to the measurements performed in perchlorate solution at various pH values. At pH 3.0 the Tafel slope in the region of interest is slightly less than 60 mV. The effect of increasing the pH is in agreement with experimental observation, i.e. as the pH is increased in the simulation the Tafel slope is decreased. In Fig. 5(b) the effect of increasing the concentration of chloride ions in the simulation of the polarization curves is seen. A similar Tafel change is observed as in the perchlorate solution when the pH was increased. The curves are in good agreement with the experiments. The Tafel slope obtained in the chloride and the perchlorate solution at pH 5 was simulated by increasing the corresponding concentration factor in the normalized rate constant. Table 3 shows the rate constants used in the simulations. In Fig. 5(a) [Cl$^-$] was kept constant
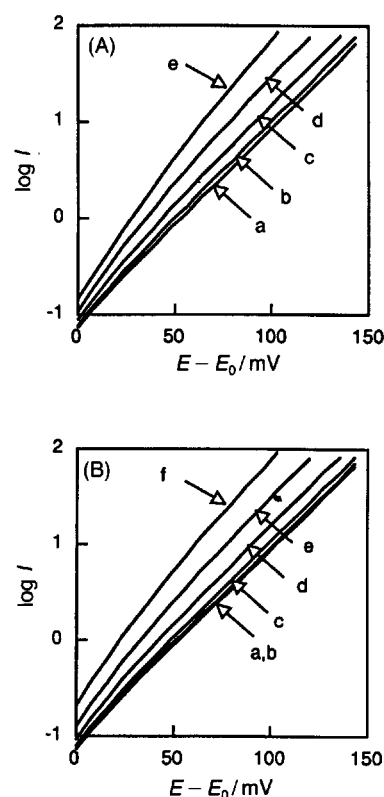

Fig. 5. Simulated polarization curves of the suggested mechanism [cf. Figs. 1(a) and (b)]. (A) Simulation of pH dependence: (a) pH 3.0, (b) 3,5, (c) 4.0, (d) 4.5 and (e) 5.0. (B) Simulation of chloride ion dependence: (a) 0, (b) 0.01, (c) 0.03, (d) 0.1, (e) 0.3 and (f) 1.0 mol dm^{-3}.

Table 3. Normalized rate constants used in the simulations.

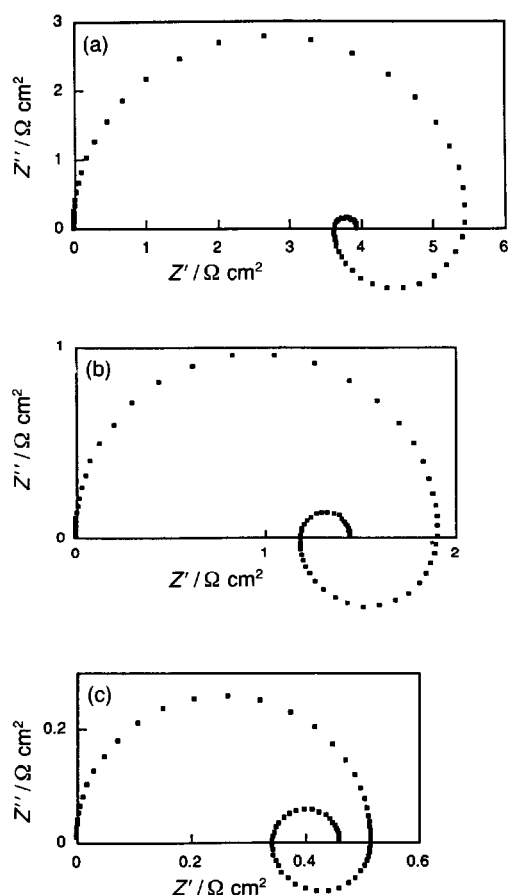| n	K_n^c/mol cm^{-2} s^{-1}	K_{-n}^c/mol cm^{-2} s^{-1}
1	1.0×10^{-8} (1 + [Cl$^-$] + 0.3 × 10^9[OH$^-$])	1.0×10^{-8} (1 + 10 × [Cl$^-$] + 10^{10}[OH$^-$])
2	1.78×10^{-8} (1 + 10 × [Cl$^-$] + 10^{10}[OH$^-$])	
3	3.28×10^{-10}	
4[a]	5.83×10^{-9}	1.0×10^{-9}

[a]Potential-independent rate constants.

Fig. 6. Simulated impedance spectra of zinc in 1 M NaClO₄ at pH 3 at three anodic potentials [cf. Figs. 2(a)–(c)]: (a) 45, (b) 65 and (c) 95 mV from the rest potential.
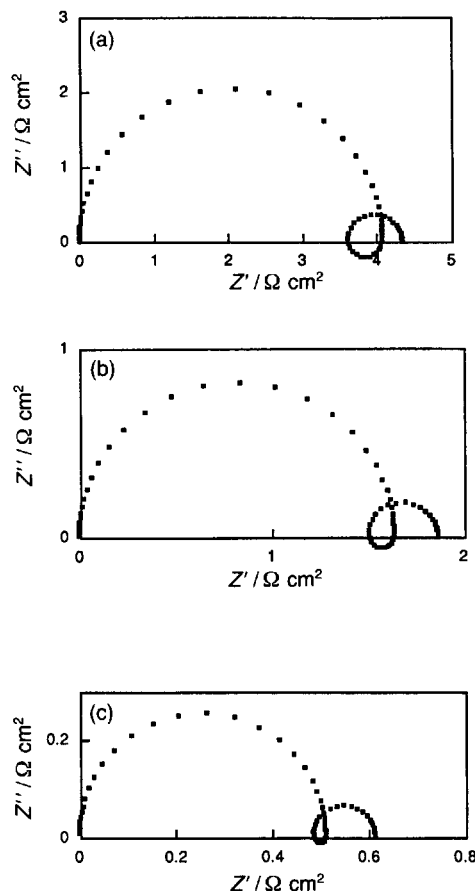

Fig. 7. Simulated impedance spectra of zinc in 1 M NaClO₄ at pH 5 at three anodic potentials [cf. Figs. 3(a)–(c)]: (a) 45, (b) 65 and (c) 95 mV from the rest potential.

at zero, while [OH⁻] was set to 10^{-11} (pH 3) and successively increased to 10^{-9} (pH 5) by two steps per decade. In Fig. 5(b) [OH⁻] was kept constant at 10^{-11} (pH 3) and [Cl⁻] was increased from 10^{-3} to 1 by two steps per decade.

In Figs. 6(a)–(c) the impedance spectra corresponding to measurements performed in NaClO₄ at pH 3.0 are shown. The simulation was performed using the same rate constants as for the simulation of the polarization behaviour at pH 3 [Fig. 5(a)]. The simulation was made at three anodic overpotentials. The spectra show reasonable agreement with experiment, except for the largest overpotential, where the capacitive loop in the low-frequency region is absent in the experimental spectrum [Fig. 2(c)]. The potential dependence of the charge-transfer resistance and the time constants associated with adsorbed intermediates show the same trends as observed in the experimental spectra.

Figs. 7(a)–(c) show the impedance spectra simulated with the hydroxide concentration set to 10^{-9} M (pH 5) and the chloride concentratioan to zero. At low overpotentials [Fig. 7(a)], the capacitive loop in the low-frequency region is somewhat smaller than the corresponding experimental loop [Fig. 3(a)]. At higher potentials [Figs. 7(b) and (c)]

there is a good correlation between simulated and experimental spectra. The potential dependence of the time constant of the inductive loop has decreased and has in fact changed sign. The corresponding experimental observation is a much weaker potential dependence at pH 5.0 than at pH 3.0. There is a small variation of τ_2 with the potential which is not seen in the experiments.

The spectra simulated with [Cl⁻] = 0 M and [OH⁻] = 10^{-11} M are shown in Figs. 8(a)–(c). The spectra show acceptable agreement with the experimental spectra. The potential dependence of both time constants, τ_1 and τ_2, shows the same trends as in the previous simulation of perchlorate solution at pH 5.

Discussion

The validity of the impedance data. Useful information can be obtained from the impedance data only if the system fulfils the following four general conditions.[20] (1) Causality: the response of the system must be caused by the input signal only. (2) Linearity: the system must show a linear response to the pertubation. (3) Stability: the system must return to its initial steady state after the perturbation. (4)
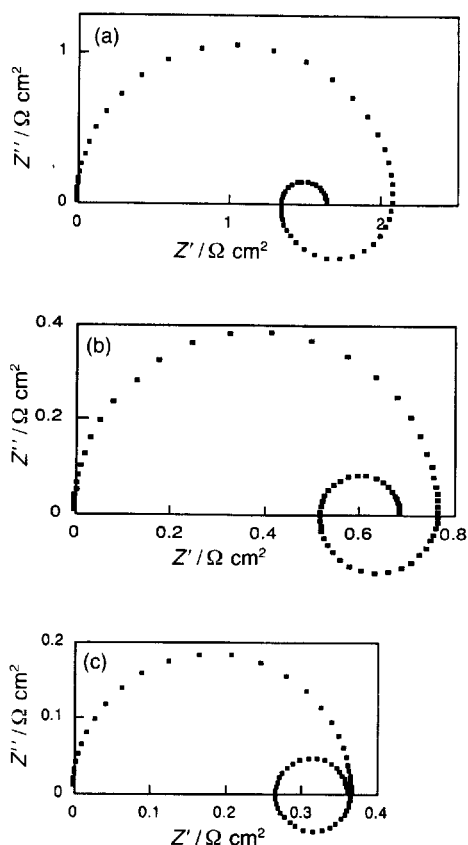
Fig. 8. Simulated impedance spectra of zinc in 1 M NaCl at pH 3 at three anodic potentials [cf. Figs. 4(a)–(c)]: (a) 40, (b) 60 and (c) 75 mV from the rest potential.

Infinity: the impedance must be finite when the frequency goes towards zero and infinity and at all intermediate frequencies.

For metal dissolution reactions, where the electrode is consumed during the measurement, the most critical condition is stability. This condition requires that the direct current remains constant during the measurement. It has been shown by Berthier et al.[21] that a double point in the impedance diagram, which is observed in the present study, may be caused by non-stationary conditions in the system. However, they also show, using a method in which the impedance data can be corrected for non-stationarity of the system[22] (simulating instantaneous impedance diagrams), that for the zinc electrode the resulting diagram conserves the double point. This indicates that the double point is not a result of any instability of the system. To confirm this further, we performed experiments where the direct current was recorded during the measurements, and it was found that the current was stable within 2 % of its magnitude. A more general test of the conditions is the application of the Kramers–Kronig transformation,[23–26] which has proved to be a valuable tool in the justification of impedance data. We have used the algorithm described by Macdonald et al.[23,24] for typical impedance spectra in this study and we have found that they transform satisfactorily.

The model. The results from the present work strongly support the presence of a catalytic step in the dissolution path of zinc. This is in agreement with earlier and similar studies made by Cachet and Wiart[15] and Deslouis et al.[16] Some of our results are, however, not in agreement with their findings, and hence a slightly different mechanism has been suggested. Possible explanations for this discrepancy may be experimental conditions (e.g. the electrolyte composition or the pre-treatment of the electrode) which differ from those reported earlier. For example, we are not able to observe the very slow relaxation of 10 mHz in the impedance spectra as reported by Cachet and Wiart[15] and Deslouis et al.[16] It has been suggested[21] that this relaxation may be due to non-stationary conditions during the measurement. Our experimental Tafel slopes lie in the interval 30–64 mV, values that we think are more reasonable than those reported in Refs. 14–16, which are considerably lower than 30 mV. It is worth noting that we have not used the Tafel coefficients b_a and b_c as fitting parameters. These coefficients have been fixed at $1/120$ mV^{-1}, except for the k_2-reaction, where $1/60$ mV^{-1} has been used in order to account for the two electrons transfered in that step. The use of extreme values of the Tafel coefficient which correspond to a transfer coefficient α, close to one or zero (as reported in some other impedance studies)[14–16,27,28] has not been necessary.

The question of whether the rate of zinc dissolution is determined by the diffusion of zinc chloro-species from the surface has been discussed in the literature.[5–7] At a stationary electrode and at high chloride concentrations it is clear that the reaction is diffusion-controlled. However, at lower chloride concentrations ($[Cl^-] \approx 1$ M]) the effect of diffusion can be eliminated by the use of a rotating-disc electrode. Cachet and Wiart[14,15] did not observe a rotation dependence on the steady-state polarization curve when the chloride concentration was as high as 4.11 M. They did, however, observe a small effect on the impedance spectra in a narrow-frequency region of the spectra, which was explained by diffusion of zinc complexes from the surface generated by the non-catalytic dissolution route. Since we have not observed any rotation dependence we consider the dissolution reaction to be totally kinetically controlled.

One argument for our suggested model is the potential dependence of the time constants associated with the adsorbed intermediates. We have in an earlier paper[17] discussed the problem of determining the true time constants from spectra with several relaxations from adsorbed intermediates. The conclusion that was drawn was that it is not possible, without assumptions concerning the separation of the time constants, to extract information about them. We have therefore extrapolated the frequency at the maximum (or minimum) of the imaginary part of the spectrum for each relaxation in order to make it possible to compare simulated data with experimental data. By using this method we observed a weaker potential dependence of the experimental and interpolated time constant associated with the Zn_{ad}^+ species when the chloride ion or hydroxide

ion concentration was increased. One way to simulate this behaviour is by changing the rate constants of the k_1^o reaction and the k_{-1}^o reaction by different amounts. This will cause the potential region where the potential dependence of the time constant of the Zn_{ad}^+ species is weak, or even zero, to move in either the anodic or cathodic direction. With this model the potential region of interest is where $k_1^o + k_3^o = k_{-1}^o$. This fact has led us to state the following hypothesis: The anions (chloride and hydroxide ions) have a greater affinity for the Zn_{ad}^+ species than for the pure zinc surface itself as well as for other intermediates. Thus the anions stimulate the k_{-1} and k_2 reaction steps (the oxidation and reduction of the Zn_{ad}^+ species) to a greater extent than the other reaction steps. Simulation of this behaviour affects the impedance spectrum and the polarization curve in the following two ways: (1) It decreases the potential dependence of both the true and the estimated time constant of the Zn_{ad}^+ species. (2) It decreases the Tafel slope at anodic potentials. This is also what is observed experimentally.

The Zn_{ad}^{+*} species is, as mentioned before, hypothetical and is introduced to explain the potential-independent relaxation found experimentally. The relevance of this species can be rationalized as an adsorbed species without an adjacent Zn atom, Zn_{kink}, which energetically favours dissolution (e.g. the regeneration of Zn_{kink} in the autocatalytic step, k_2, is for some reason hindered). For a polycrystalline zinc surface a large number of steps and kinks are available. Intermediates at these sites have higher energy than intermediates located at other places such as the plane surface or blocked steps or kinks. A blocked step or kink may be considered as one unable to form a new kink upon the desorption of the intermediate and the simultaneous regeneration of a new intermediate. Upon oxidation Zn_{ad}^+ is formed and can, if it is adjacent to an active zinc atom in the lattice, be oxidized further through the catalytic path. Suppose that an active zinc atom is not available; the Zn_{ad}^+ species will then relax and further oxidation will thus follow the non-catalytic path. On a smooth surface, e.g. amalgamated zinc, one would expect the non-catalytic path to dominate, since the surface is more homogeneous. Experimentally this is also indicated, and further studies along this line are under evaluation.

The use of the product R_pI *or* R_tI *in the Tafel analysis.* It was shown in a previous paper[17] that when chemical steps become important for the rate of an electrochemical reaction the simple and inverse relationship between the polarization resistance and the steady-state current disappears. This has some implications in the analysis of our suggested model. From our Tafel, R_t and R_p analysis of different mechanisms the following can be stated about the catalytic mechanism when the non-catalytic path is slow. If the mechanism is simulated without the presence of anions the Tafel slope is, with $\alpha = 1/2$, 60 mV in the potential region of interest. Note that the first step is not in equilibrium. Non-equilibrium conditions of the first step are necessary

for inductive behaviour of the Zn_{ad}^+ species. If the presence of anions is simulated by increasing the rate constants k_2^o and k_{-1}^o, the coverage of Zn_{ad}^+ will decrease and the Tafel slope will change from 60 towards 30 mV. An interesting observation is, however, that, although the potential region where the Tafel slopes change from 30 to 60 mV is moved in the anodic direction by this simulation, the product R_tI still remains constant at 60 mV/ln 10 in the potential region where the Tafel slope has decreased. This means that under these conditions R_tI cannot be used to estimate the Tafel slope for this mechanism. Neither can the product R_pI be used to estimate the Tafel slope, since the relaxation of Zn_{ad}^{+*} species, generated by the chemical step in the non-catalytic path, has a significant contribution to the polarization resistance in this potential region.

Conclusions

(1) The main dissolution route of zinc in slightly acidic perchlorate and chloride solutions is autocatalytic. (2) In parallel a non-catalytic path takes place, yielding a potential-independent relaxation in the impedance diagram. (3) The effect of hydroxide and chloride ions is explained by a destabilization of the Zn_{ad}^+ intermediate.

References

1. Morgan, S. W. K. *Zinc and its Alloys and Compounds* Ellis Horwood, Chichester 1985.
2. Van Ooij, W. J., Sabata, A. and Ström, G. *Progr. Organic Coatings 18* (1990) 147.
3. Van Ooij, W. J., Anderson, H. and Ström, G. *Paper No. 51 at NACE Corrosion 88,* St Louis, MI (1988).
4. Blackledge, J. and Hush, N. S. *J. Electroanal. Chem. 5* (1963) 435.
5. Hurlen, T. *Acta Chem. Scand. 16* (1962) 1337.
6. Hurlen, T. *Acta Chem. Scand. 16* (1962) 1346.
7. Hurlen, T. *Acta Chem. Scand. 16* (1962) 1353.
8. Hurlen, T. and Eriksrud, E. *J. Electroanal. Chem. 45* (1973) 405.
9. Hurlen, T. and Fischer, K. P. *J. Electroanal. Chem. 61* (1975) 165.
10. Gaiser, L. and Heusler, K. E. *Electrochim. Acta 15* (1970) 161.
11. Heusler, K. E. and Knödler, R. *Electrochim. Acta 18* (1973) 855.
12. Heusler, K. E. *Z. Elektrochem. 62* (1958) 582.
13. Baugh, L. M. *Electrochim. Acta 24* (1979) 657.
14. Cachet, C. and Wiart, R. *J. Electroanal. Chem. 111* (1980) 235.
15. Cachet, C. and Wiart, R. *J. Electroanal. Chem. 129* (1981) 103.
16. Deslouis, C., Depart, M. and Tournillon, C. *Corros. Sci. 29* (1989) 13.
17. Ahlberg, E. and Anderson, H. *Acta Chem. Scand. 46* (1992) 1.

18. Kendig, M. W., Allen, A. J. and Mansfield, F. *J. Electrochem. Soc. 131* (1984) 935.
19. Ahlberg, E. and Friel, M. *Electrochim. Acta 34* (1989) 1523.
20. Macdonald, J. R. *Impedance Spectroscopy*, John Wiley & Sons, New York 1987.
21. Berthier, F., Diard, J. P., Jussiaume, A. and Rameau, J. *J. Corros. Sci. 30* (1990) 239.
22. Stoynov, Z. and Sovova, B. *J. Electrochem. Soc. 112* (1980) 157.
23. Macdonald, D. D. and Urquidi-Macdonald, M. *J. Electrochem. Soc. 132* (1985) 2316.
24. Macdonald, D. D. and Urquidi-Macdonald, M. *J. Electrochem. Soc. 133* (1986) 2018.
25. Macdonald, D. D. and Urquidi-Macdonald, M. *J. Electrochem. Soc. 137* (1990) 515.
26. Urquidi-Macdonald, M., Real, S. and Macdonald, D. D. *Electrochem. Acta 35* (1990) 1559.
27. Macdonald, D. D., Real, S., Smedley, S. and Urquidi-Macdonald, M. *J. Electrochem. Soc. 135* (1988) 2397.
28. Epelboin, I. and Keddam, M. *J. Electrochem. Soc. 117* (1970) 1052.